Electronic Supplementary Material (ESI) for Journal of Materials Chemistry C.

Supporting Information for

Preparation of Soft Somatosensory-detecting Materials via Selective Laser Sintering

Siqi Wei[a], *Lijing Zhang*[a], *Chong Li*[a], *Shengyang Tao**[a], *Baojun Ding*[a], Huichao Zhu[b] and Shufeng Xia[b]

[a]Department of Chemistry, School of Chemical Engineering, Dalian University of Technology, Dalian 116024, China

*E-mail: taosy@dlut.edu.cn

[b]College of Electronic Science and Technology, Dalian University of Technology, Dalian 116024, China

Supporting Information

Finite element analysis of temperature during laser sintering:

A laser beam (laser power record as P) moves forward on the PA12 powder bed with a scanning speed of v (100 mm·s^{-1}). The transient thermal response of the surface of the powder bed can be obtained by simulating the heat source of the surface of the powder bed by the incident heat flux of the laser.

The surface emissivity of the powder bed is ε. It is assumed that the absorption rate is equal to the emissivity during the operating wavelength range of the laser. Therefore, the thermal load generated by the laser should be multiplied by ε. Also, the powder bed is considered opaque with no light penetrates the powder bed in the operating wavelength range of the laser. Thus, all the heat generated by the laser is acted on the surface of the powder bed.

According to the energy conservation law:

$$\rho C_{\mathrm{p}} \frac{\partial \mathrm{T}}{\partial \mathrm{t}} + \rho C_{\mathrm{p}} u \cdot \nabla T + \nabla \cdot q = Q + Q_{\mathrm{ted}} \qquad \text{(eq. S1)}$$

where ρ is density, Cp is the constant pressure heat capacity, T is temperature, t is time. Heat flux q (W·m^{-2}) is defined as: $q = -\kappa \nabla T$, here κ (W·m^{-1}k^{-1}) is heat conductivity. Heat flux of the surface of the powder bed: $q_0 = \varepsilon \times q$.

Supporting Figures

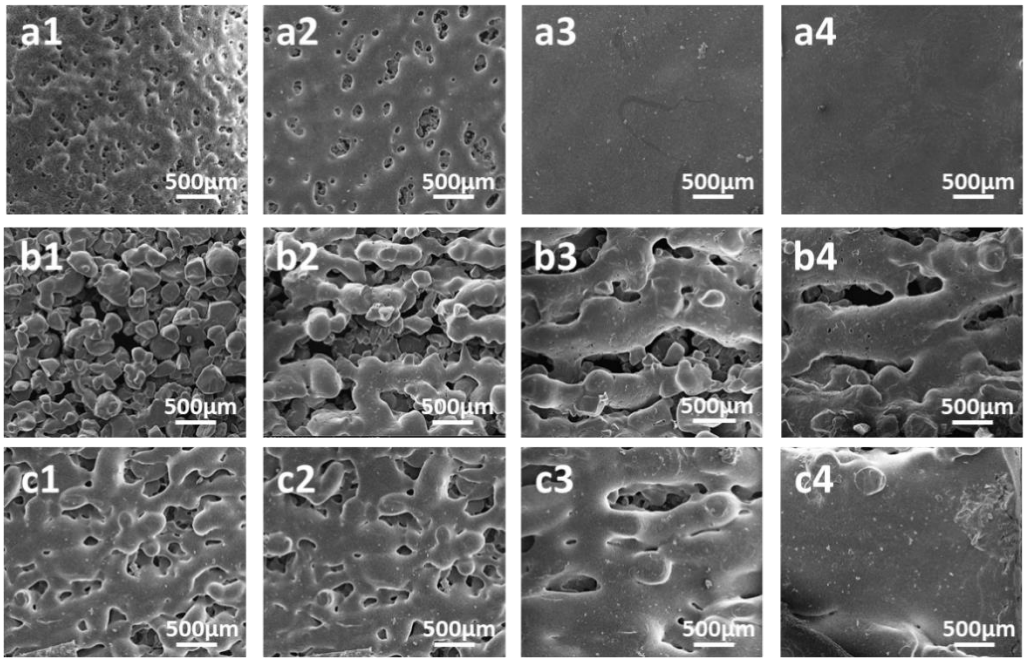

Figure S1. SEM image of PA12 (a1-a4), PP(b1-b4), and TPU(c1-c4) film prepared under different laser power: 1.5 W, 1.8 W, 2.1 W, 2.4 W.

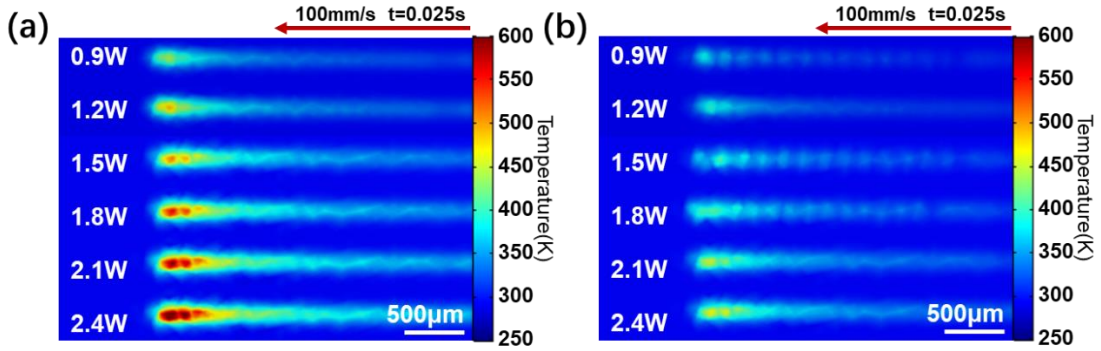

Figure S2. Finite element analysis of laser sintering temperature under different power (a and b are PP and TPU respectively).

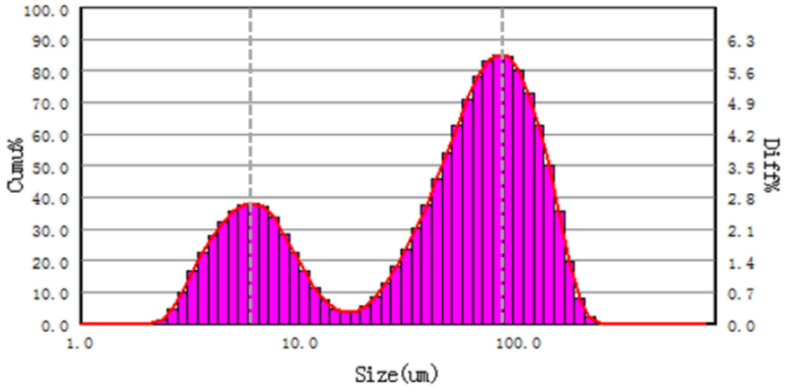

Figure S3. Particle size distribution of graphite/PA12 missed powder after ball milling with a milling speed of 1500 rpm for 20 min.

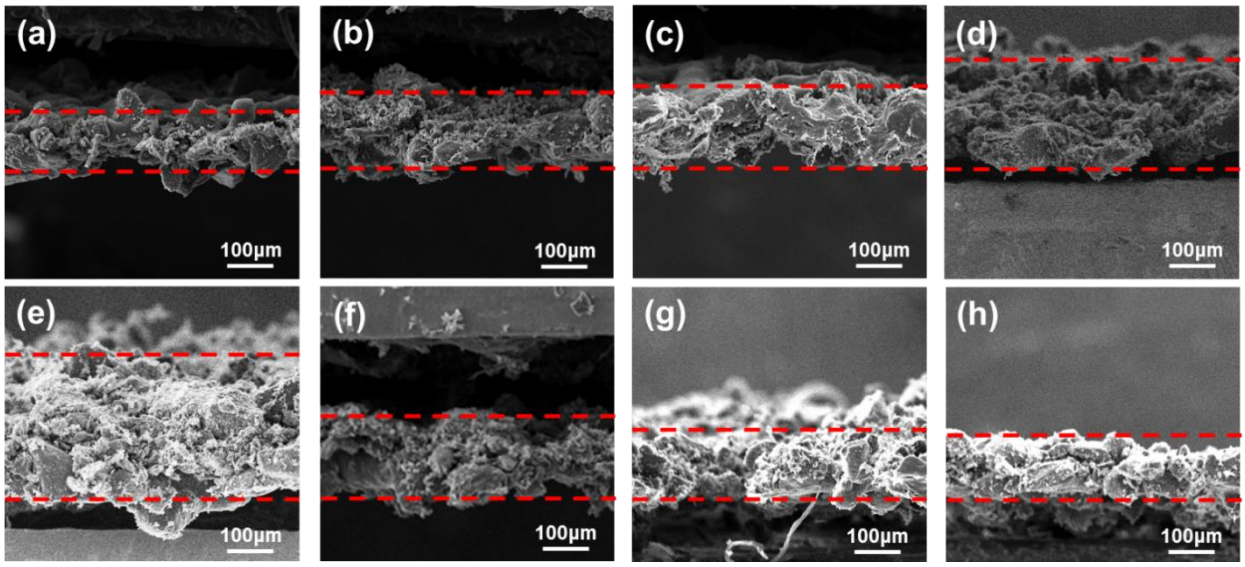

Figure S4. Thickness of graphite/PA12 film prepared under different preparation conditions. Cross-section of graphite/PA12 film prepared under (a-d) different laser power (a-d are 1.5 W, 1.8 W, 2.1 W, 2.4 W respectively, filling space is 0.10 mm); (e-h) different filling space (e-h are 0.06 mm, 0.10 mm, 0.14 mm, 0.18 mm respectively, laser power is 1.8 W).

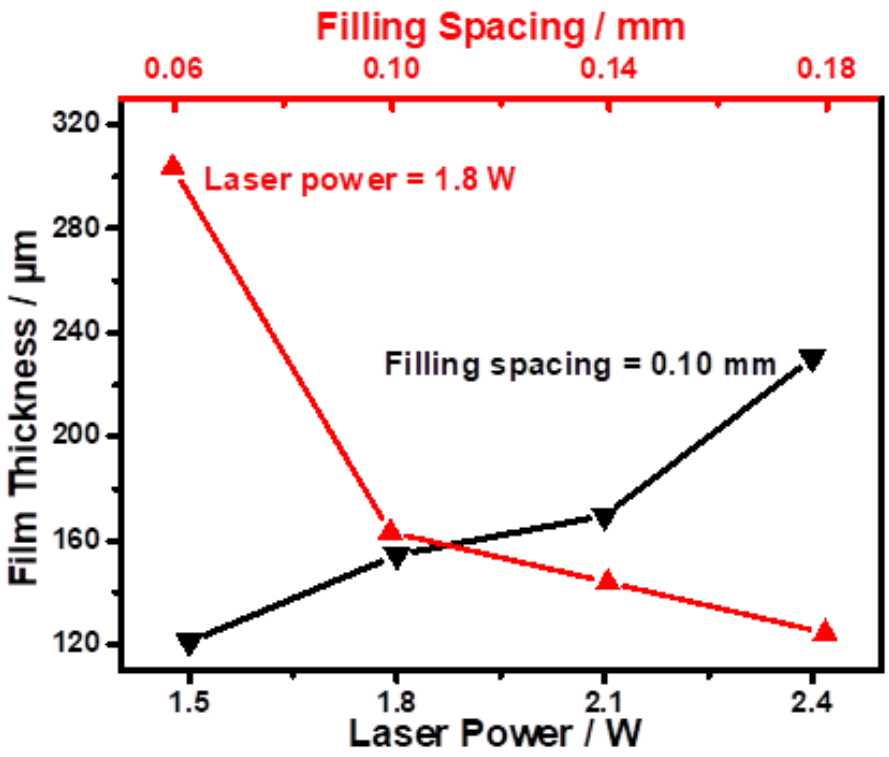

Figure S5. The thickness of graphite/PA12 film prepared under different preparation conditions.

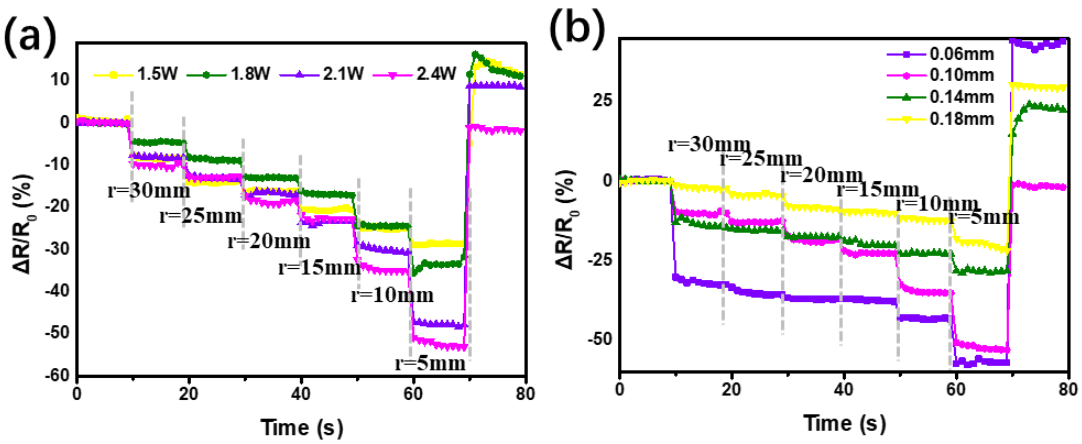

Figure S6. Bending sensing properties of the upper surface of graphite/PA12 films. The resistance increased ratio $\Delta R/R_0$ (%) of graphite/PA12 film versus (a) laser power, and (b) filling space. The sensitivity increased naturally as the laser power increased. The high laser power of 2.4 W led to a high sintering temperature which facilitated the fusion of the PA12 powder and improved the repeatability of the sensor. As the filling spacing reduced, the response intensity of the film increased. The small filling spacing reduced the distance between two laser-scanning paths and increased the connection of the PA12 to reduce pores. However, a tiny filling space of 0.06 mm leading to the over-sintering of the film, so the irreversible damage might emerge. Therefore, the sintering power of 2.4 W and the filling spacing of 0.10 mm was used for the preparation of the SDM to detect the bending stimulation.

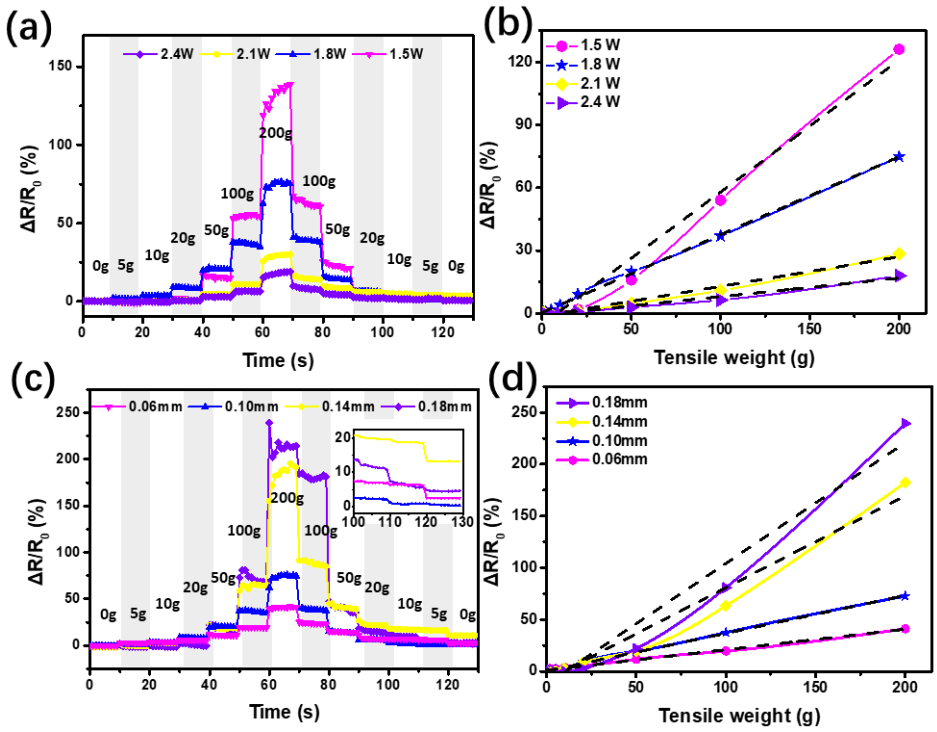

Figure S7. Tensile strength sensing properties of the graphite/PA12 films. The resistance increased ratio $\Delta R/R_0$ (%) of graphite/PA12 film prepared under (a, b) different laser power and (c, d) different filling spacing. Dash lines are linear regressions corresponding to the sensor sensitivity (SS) of each material. SS increased as the filling spacing get larger. The too large filling spacing decreased the ability of the sensor to return to the initial resistance after stretching, the linearity of tensile strength sensing was also be affected (R^2 decreased from 0.99 to 0.95 as the filling spacing increased from 0.06 mm to 0.18 mm); the increasing of laser energy led to the increase of the thickness of graphite/PA12 film and the enhancement of its mechanical strength, which promoted the repeatability and reduced the SS value. Therefore, tensile strength sensor was prepared under the laser power of 1.8 W and the filling space of 0.10 mm.

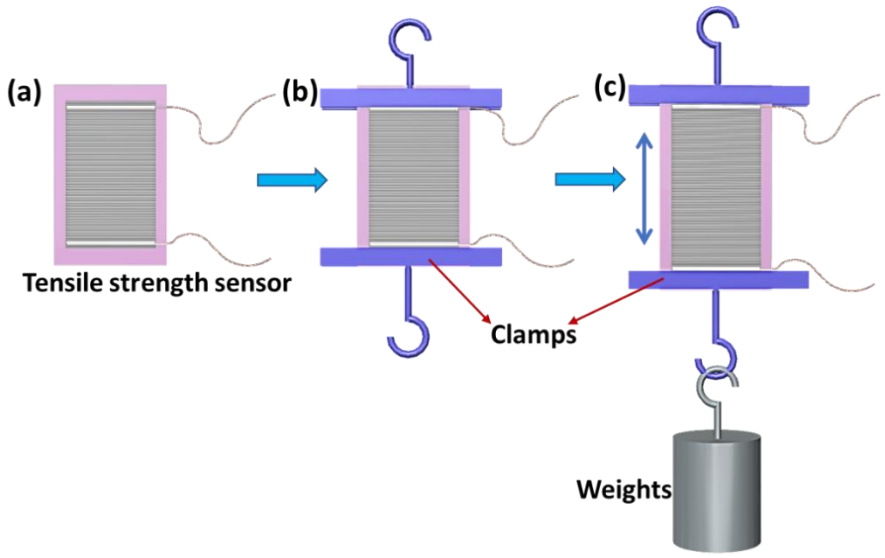

Figure S8. Schematic of the test equipment for investigating the tensile response of the graphite/PA12 film. The sensor was fixed by two clamps and hung vertically, then the weights of different quality were hung below to provide tension of different value.

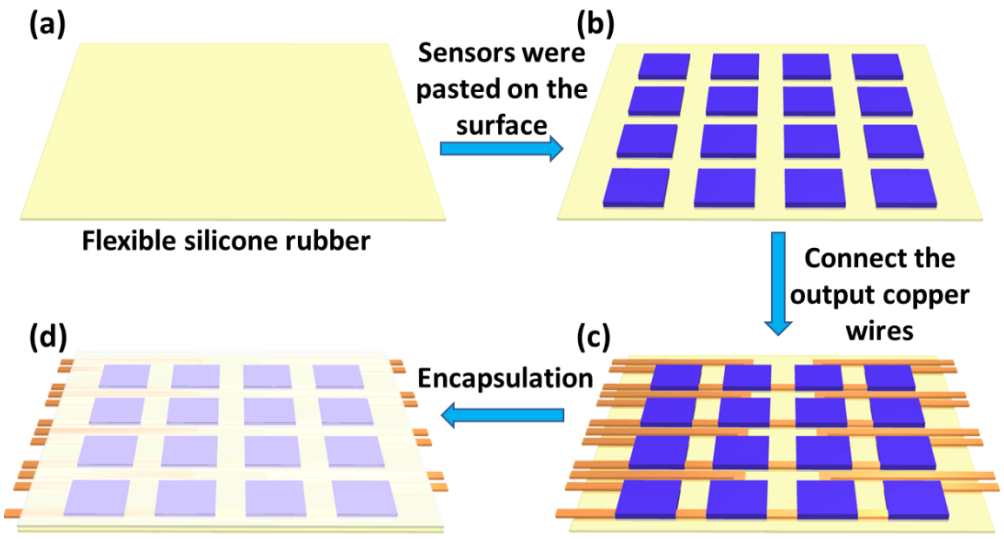

Figure S9. Fabrication processes of the graphite/PA12 pressure sensor matrix. Firstly, the flexible silicone rubber mat was chosen as the substrate of the sensor matrix, and then the graphite/PA12 sensors were pasted thereon by a thin layer of tape. Afterward, the output copper wires were connected to the sensor with silver paste. Finally, the sensor matrix was encapsulated with a PDMS film.

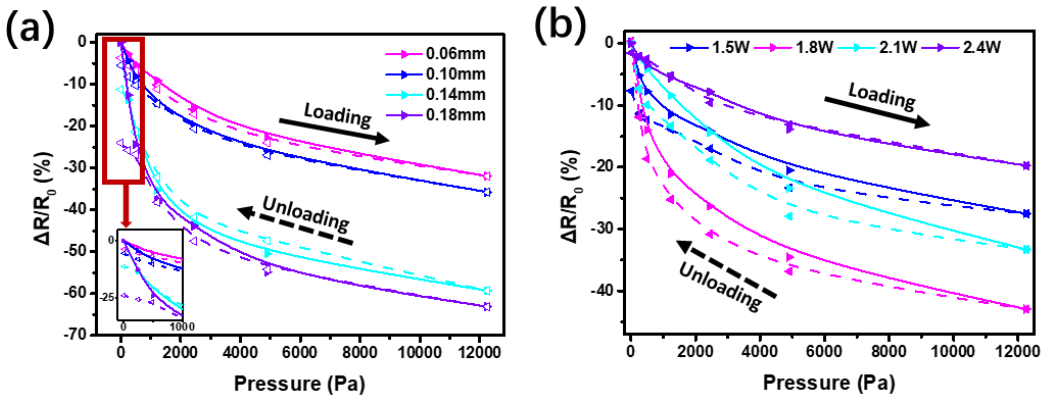

Figure S10. Pressure sensing properties of the PA12/graphite films. The resistance increased ratio $\Delta R/R_0$ (%) of PA12/graphite film versus a) filling spacing and b) laser power.

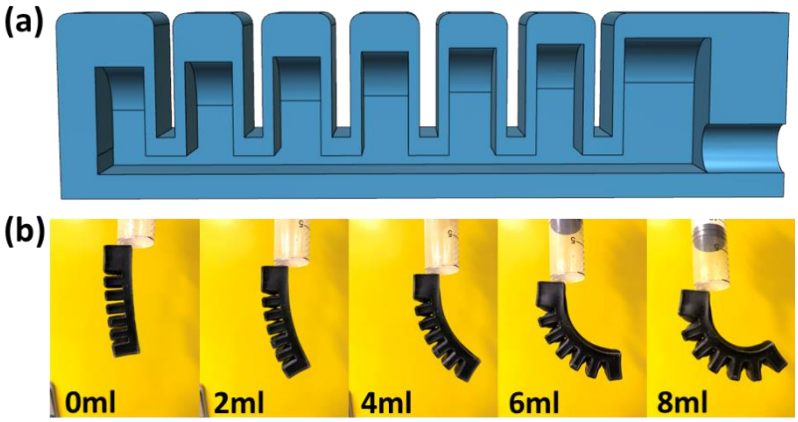

Figure S11. a) Cross-section diagram of the soft pneumatic actuator, b) Actuation experiment of soft pneumatic actuator under inputting air volume of 0 ml, 2 ml, 4 ml, 6 ml, 8 ml respectively.

Supporting Tables

Table S1. Sintering conditions of different polymer particles sintered under different laser power.

Laser power/W	**0.9**	**1.2**	**1.5**	**1.8**	**2.1**	**2.4**
TPU	Thin, weak	Deformation in evident with the increased laser power, and the edges warped				
PA12	—[(a)]	Thin	Well mechanical strength		Light yellow, weak deformation	
PP	—	Poor mechanical strength, Rough surface		Edges warped		

(a) "—" indicates that film cannot be formed.

Table S2. Strain sensing properties of the graphite/PA12 films. Corresponding sensor sensitivity (SS) and R^2 of a strain sensor in figure S7(b) and (d).

Filling Space	SS ($\times 10^{-1}$)	R^2	Laser Power	SS ($\times 10^{-1}$)	R^2
0.18 mm	11.66	0.95	1.5 W	6.31	0.98
0.14 mm	8.88	0.96	1.8 W	3.72	0.99
0.10 mm	3.65	0.99	2.1 W	1.41	0.98
0.06 mm	1.98	0.99	2.4 W	0.89	0.97

Table S3. Corresponding weight and radius of the objects grabbed by the soft robotic gripper.

Object	Weight/g	Radius/mm
3D printed ball	19.5	22.6
Egg	51.6	21.0
Nut	16.0	16.4
Kumquat	25.3	12.9

Supporting Movies

Movie S1. Pressure and bending sensor in real-time monitoring of the motions of the soft gripper. The movie shows the simultaneous response of the pressure and bending sensors to the corresponding motions when the soft gripper grabs different objects (including 3D printed ball, egg, nut, and kumquat). Corresponding weight and radius of the objects were showed in Table S3. The response signal pattern of each motion was extracted and demonstrated in Figure 10.